Journal of Power Sources 224 (2013) 93–98

Contents lists available at SciVerse ScienceDirect

Journal of Power Sources

journal homepage: www.elsevier.com/locate/jpowsour

# Characterization of N-butyl-N-methyl-pyrrolidinium bis(trifluoromethanesulfonyl)imide-based polymer electrolytes for high safety lithium batteries

Jae-Kwang Kim [a,*], Leszek Niedzicki [b], Johan Scheers [a], Cho-Rong Shin [c], Du-Hyun Lim [c], Wladyslaw Wieczorek [b], Patrik Johansson [a], Jou-Hyeon Ahn [c], Aleksandar Matic [a,**], Per Jacobsson [a]

[a] Department of Applied Physics, Chalmers University of Technology, 412 96 Göteborg, Sweden
[b] Polymer Ionics Research Group, Faculty of Chemistry, Warsaw University of Technology Noakowskiego 3, PL-00664 Warsaw, Poland
[c] Department of Chemical & Biological Engineering and Engineering Research Institute, Gyeongsang National University, 900 Gajwa-dong, Jinju 660-701, Republic of Korea

## HIGHLIGHTS

- PVdF-HFP membrane was prepared by electrospinning.
- $Py_{14}TFSI$-based gel polymer electrolyte has good physical properties.
- $Py_{14}TFSI$-based gel polymer electrolyte shows excellent electrochemical properties.

## ARTICLE INFO

*Article history:*
Received 7 April 2012
Received in revised form
28 July 2012
Accepted 10 September 2012
Available online 29 September 2012

*Keywords:*
Polymer electrolyte
Electrospinning
N-butyl-N-methyl-pyrrolidinium bis(trifluoromethanesulfonyl)imide
Poly(vinylidene difluoride-*co*-hexafluoropropylene)
Lithium batteries

## ABSTRACT

Poly(vinylidene difluoride-*co*-hexafluoropropylene) (PVdF-HFP) membrane was prepared by electrospinning. The membranes served as host matrices for the preparation of ionic liquid-based polymer electrolytes (ILPEs) by activation with non-volatile, highly thermally stable, and safe room temperature ionic liquid (RTIL) electrolytes; N-butyl-N-methyl-pyrrolidinium bis(trifluoromethanesulfonyl)imide ($Py_{14}TFSI$) complexed with 1 M lithium bis(trifluoromethanesulfonyl)imide (LiTFSI). In this work, the first combination of electrospun PVdF-HFP fiber polymer host and pyrrolidinium-based ionic electrolyte was employed for highly stable lithium batteries. The ILPE exhibited low $Li^+$—TFSI coordination, low crystallinity, high thermal stability, high electrochemical stability, and high ionic conductivity with a maximum of $1.1 \times 10^{-4}$ S $cm^{-1}$ at 0 °C. The ILPE exhibited good compatibility with a $LiFePO_4$ electrode on storage and good charge–discharge performance in Li/ILPE/$LiFePO_4$ cells at room temperature, delivering specific capacities of 143 and 115 mA h $g^{-1}$ at 0.1 and 1 C-rates. The ILPE also exhibited stable cycle properties and have therefore been demonstrated to be suitable for lithium battery applications.


## 1. Introduction

Lithium polymer batteries have received considerable attention in recent years since they offer versatility of shape, flexibility, lightness, and are intrinsically safe. Thus, they can be commercialized in miniature electronic device, as well as electric vehicles [1]. However, suitable polymer electrolytes must satisfy the following properties: high ionic conductivity, good mechanical, thermal, interfacial, and electrochemical stabilities.

Among the polymer electrolytes suggested for lithium batteries, polyethylene oxide (PEO) has been widely studied as a promising host polymer, because of the good thermal properties and interfacial stability. However, due to a high degree of crystallinity, PEO-based polymer electrolytes have very low ionic conductivities below room temperature [2,3]. Efforts have been made to increase the ionic conductivity at low temperatures, where plasticized or gel polymer electrolytes have attracted much attention, since they show high ionic conductivity at room temperature by immobilizing large amounts of liquid electrolyte in a polymer host [4–6]. The polymer hosts are membranes adapted specifically for the plasticized or gel polymer electrolytes with pores of nanometer to micrometer size that retain the liquid electrolyte. The membranes should have the capability to absorb the liquid electrolyte without leakage, be chemically compatible with electrode materials, and

* Corresponding author. Tel.: +46 31 772 3352; fax: +46 31 772 2096.
** Corresponding author.
*E-mail addresses:* jaekwang@chalmers.se (J.-K. Kim), matic@chalmers.se (A. Matic).

0378-7753/$ – see front matter © 2012 Elsevier B.V. All rights reserved.
http://dx.doi.org/10.1016/j.jpowsour.2012.09.029

adhere well to the electrode. We prepared polymer membranes by an electrospinning process. The electrospun membranes appear to be particularly suitable as host matrices in microporous polymer electrolytes, because the fully interconnected pores have large surface areas that can function as efficient channels for ion conduction [6–8]. Among the few polymers for membranes that meet the necessary requirements is poly(vinylidene difluoride-*co*-hexafluoropropylene) (PVdF-HFP), which has a strong electron withdrawing function, a unique arrangement and a high dielectric constant. Thus, effectively dissociating lithium salts to generate a large quantity of charge carriers for conduction. Apart from the diffusion established by a plasticizer, such as ionic liquid electrolytes, it is highly likely that conduction occurs also through the swollen PVdF-HFP host, which makes this a very suitable host.

At present, room temperature ionic liquids (RTILs) are considered the most promising plasticizers to substitute for the organic solvents of lithium batteries. Consisting of an organic cation and an inorganic anion, RTILs have several advantages over organic solvents: high chemical and thermal stability, non-flammability, and negligible vapor pressure. In some cases also high electrochemical stability and hydrophobicity [9,10]. In addition, the use of RTILs in less controlled environments than ultra-dry, oxygen-free glove boxes would certainly benefit industrial electrochemical processes. An example of this type of RTIL is N-butyl-N-methylpyrrolidinium bis(trifluoromethanesulfonyl)imide ($Py_{14}TFSI$), which is stable in air, has a sub-ambient melting temperature, high ionic conductivity, and a wide electrochemical window. It generates a superoxide ion in the cathodic process and forms a solid electrolyte interface (SEI) that prevents undesired reactions between the carbon anode and electrolyte [10–14].

Here we have investigated the electrochemical performance of $LiFePO_4$ cathodes working together with the ionic liquid-based polymer electrolytes, since $LiFePO_4$ is inexpensive, non-toxic, thermally stable, and has a high specific capacity (170 mA h $g^{-1}$) [15,16]. Several research groups have already studied PVdF-HFP-based plasticized ionic liquid polymer electrolytes prepared by phase inversion and PEO-based ionic liquid polymer electrolyte for $LiFePO_4$ batteries [17–21]. However, for these polymer electrolytes physical and electrochemical properties, such as ion paring, ionic conductivity, low temperature stability, and electrochemical stability can still be improved. The ionic liquid-based polymer electrolyte (hereafter named ILPE) composited with a PVdF-HFP electrospun fiber membrane and $Py_{14}TFSI$, shows high electrochemical and thermal stability, and high cycling stability. Also, in particular, a high ionic conductivity showed at low temperatures.

## 2. Experimental

$Py_{14}TFSI$ and lithium bis(trifluoromethanesulfonyl)imide (LiTFSI) were both obtained from Aldrich (≥99% purity), stored under Argon atmosphere, and used as received. The moisture content of 1 M LiTFSI in $Py_{14}TFSI$ was measured by coulometric Karl Fischer titration to be 100 ppm. The value could not be sufficient but an influence was not discovered on this study. The PVdF-HFP fibrous membrane was prepared by electrospinning according to the method described previously [6,8]. A 16 wt.% solution of PVdF-HFP (Kynar Flex 2801) in a mixed solvent of acetone and N,N-dimethylacetamide (HPLC grades, Aldrich) in 7:3 wt. ratio was electrospun at room temperature. A homogenous film of ~80 μm thickness was obtained. The membrane has a porous structure of entwined polymer fibers of ~1.5 μm average thickness, forming a net with a mesh size of ~5 μm. The ILPE was obtained by soaking the polymer membrane for 10 s in a solution of 1 M LiTFSI/$Py_{14}TFSI$ (mol $L^{-1}$) under argon atmosphere at room temperature. The weight ratio of polymer membrane and IL is 1:3.

Membrane electrolyte uptake was determined by soaking a circular piece of the membrane (diameter 1.6 cm) in ionic liquid electrolyte (ILE). The weight of the wetted membrane was determined at different soaking intervals, taking care to remove excess electrolyte remaining on the surface of the membrane by wiping softly with tissue paper. The electrolyte uptake ($\varepsilon$) was calculated using the relation:

$$\varepsilon(\%) = \frac{M - M_0}{M_0} \times 100$$

where $M_0$ is the mass of the dry PVdF-HFP membrane and $M$ is the mass after soaking with ILE. The ILE uptake of the fibrous PVdF-HFP membrane in the present study is much higher (~300%) compared to that reported for Celgard separators (~130%) [7]. The $LiFePO_4$ cathode material, with 6 wt.% carbon coating, was prepared by a mechanical activation process under optimized condition [15,22].

Raman spectra of the ionic liquids and the ionic liquid electrolytes were recorded on a Bruker IFS66 Fourier Transform spectrometer, equipped with an FRA 106 Raman module and using the 1064 nm line of a Nd:YAG laser as excitation source. The laser power was set to 250 mW and the resolution was 4 $cm^{-1}$. $^7Li$ NMR measurements were performed using a Bruker DSX-300 solid state NMR spectrometer at room temperature. Differential scanning calorimetry (DSC) experiments were performed using a Q1000 from TA Instruments at a heating rate of 10 °C $min^{-1}$ and a helium flow rate of 25 mL $min^{-1}$. The samples were sealed in aluminum DSC pans inside an argon atmosphere glove box ($H_2O$ <10 ppm). Typically the samples were first cooled at a rate of 20 °C $min^{-1}$ from 40 °C to −140 °C and then heated at 10 °C $min^{-1}$ to 180 °C. The ionic conductivity of the ionic liquid-based electrolytes was measured from −70 °C to 80 °C in a gold-plated cell, over the frequency range $10^{-1}$–$10^6$ Hz, using a Novocontrol broadband dielectric spectrometer. Thermal gravimetric analysis (TGA) of the samples was performed on an SDT-Q600 (USA) instrument under oxygen flow and at a heating rate of 10 °C $min^{-1}$.

Lithium transference numbers ($t_+$) were measured using the D.C. polarization method with Bruce and Vincent correction [23,24]. The frequency range for the EIS measurements was 500 kHz–100 mHz, with a 10 mV ac signal. Polarization was performed with a 20 mV dc signal. The lithium cation transference numbers were calculated as:

$$t_+ = \frac{I_S(\Delta V - R_0 I_0)}{I_0(\Delta V - R_S I_S)}$$

where $\Delta V$ is the polarization potential (20 mV); $R_0$ is the interfacial resistance of the lithium electrode before polarization; $R_s$ is the interfacial resistance of the lithium electrode after polarization; $I_0$ is current at the start of polarization, and $I_s$ is the steady-state current at polarization. The steady-state technique may be applied when the Li electrode/electrolyte interface resistance is negligible [23,25].

Every material was evaluated in three independently assembled samples. The cell assembly was made in glove box with oxygen and moisture level of below 1 ppm. Lithium electrodes were provided by Sigma–Aldrich (Lithium ribbon, 99.9% trace metal basis). All measurements were performed on a VMP3 multichannel potentiostat-galvanostat (Bio-Logic Science Instruments, France).

For the electrochemical measurements $LiFePO_4$ powder, carbon black and poly(vinylidene difluoride) (PVdF: Aldrich) binder were added to N-methyl pyrrolidone (NMP) solvent in the ratio 83:7:10, by weight. The viscous slurry was cast on aluminum foil and dried at 95 °C under vacuum for 12 h. The film was cut into circular discs of area 0.95 $cm^2$ and mass ~3.0 mg for use as cathodes. Cyclic voltammetry (CV) measurements of Li/ILPE/Li cells were performed at a scan rate of 1 mV $s^{-1}$, between −1 and +1 V. Electrochemical

stability was determined by linear sweep voltammetry (LSV) of Li/ILPE/SS cells at a scan rate of 1 mV $s^{-1}$ at 25 °C. Electrochemical performance tests of $LiFePO_4$/ILPE/Li cells were carried out using an automatic galvanostatic charge–discharge unit, a WBCS3000 battery cycler, between 2.5 and 4.0 V. These experiments were performed at 0.1 (0.042 mA $cm^{-1}$) and 1 (0.42 mA $cm^{-1}$) C current density rates.

## 3. Results and discussion

Fig. 1 displays the ionic conductivity of the ILE and ILPE as a function of temperature. As expected, the ionic conductivity of both electrolytes drops at decreasing temperature and shows the Vogel–Fulcher–Tammann (VFT) behavior normally observed in amorphous ionic conductors [21,26]. The comparison shows that the conductivity of the ILPE is almost equal to the ILE in the temperature region from −40 to 70 °C. However, below these temperatures the ILPE conductivity is higher. The low temperature ionic conductivity of the ILPE is more than 4 orders of magnitude higher than for the ILE in the temperature range from −50 to −70 °C. Obviously, the inhibition of phase transition and crystallization of ILPE compensate for the low ionic mobility otherwise imposed by the polymer matrix at these temperatures. This result is in good agreement with the thermal investigation of Fig. 2. The ionic conduction, coupled to the mobility and the concentration of free charge carriers, increases over the entire temperature range examined compare to other published $Py_{14}$TFSI-based polymer electrolytes [21,27,28]. Inseted figure shows the morphology of the electrospun PVdF-HFP membrane obtained by SEM. The membrane has a homogeneous distribution of nano-fibers with diameters around 1.5 μm.

Fourier transforms Raman spectroscopy (FT-Raman) is a useful technique for studying local structural changes and different conformers of the $TFSI^-$ anion. Raman spectra were recorded for the pure ILE (1 M LiTFSI in $Py_{14}$TFSI) and ILPE in Fig. 2a. The two spectra are similar, due to the $Py_{14}^+$ cation and the $TFSI^-$ anion, with to be main features indicated in the figure. The peaks originating from PVdF-HFP at 796, 879, 960, 1062, 1187, and 1363 $cm^{-1}$ correspond to the $CF_3$ group, $CH_2$ rocking, $CH_2$ vinylidene wagging, out of plane C–H bonding, symmetric C–F stretching, $CF_2$ stretching, symmetrical stretching $CF_3$, $CH_2$ wagging, and a scissoring vibration of vinylidene. The peak at 1062 $cm^{-1}$ is a signature of the crystalline phase of PVdF-HFP [29]. Fig. 2b shows the two conformers of $TFSI^-$ anion and the $Li^+$ coordinated TFSI in the

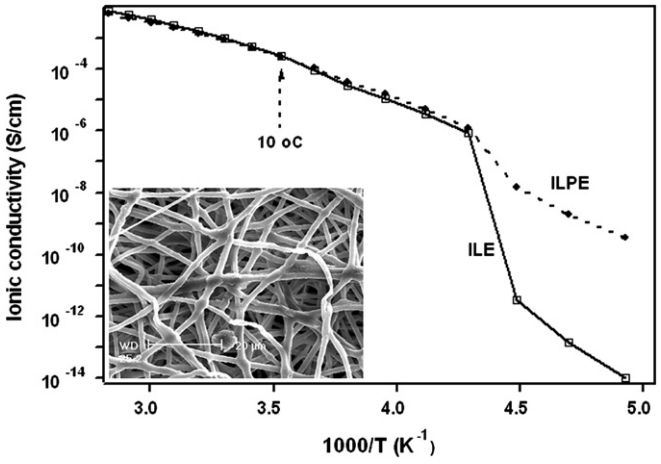


**Fig. 1.** Ionic conductivity as a function of temperature for the $Py_{14}$TFSI ionic liquid electrolyte (ILE) and the $Py_{14}$TFSI-based polymer electrolyte (ILPE). Inseted figure is SEM image of electrospun PVdF-HFP membrane.

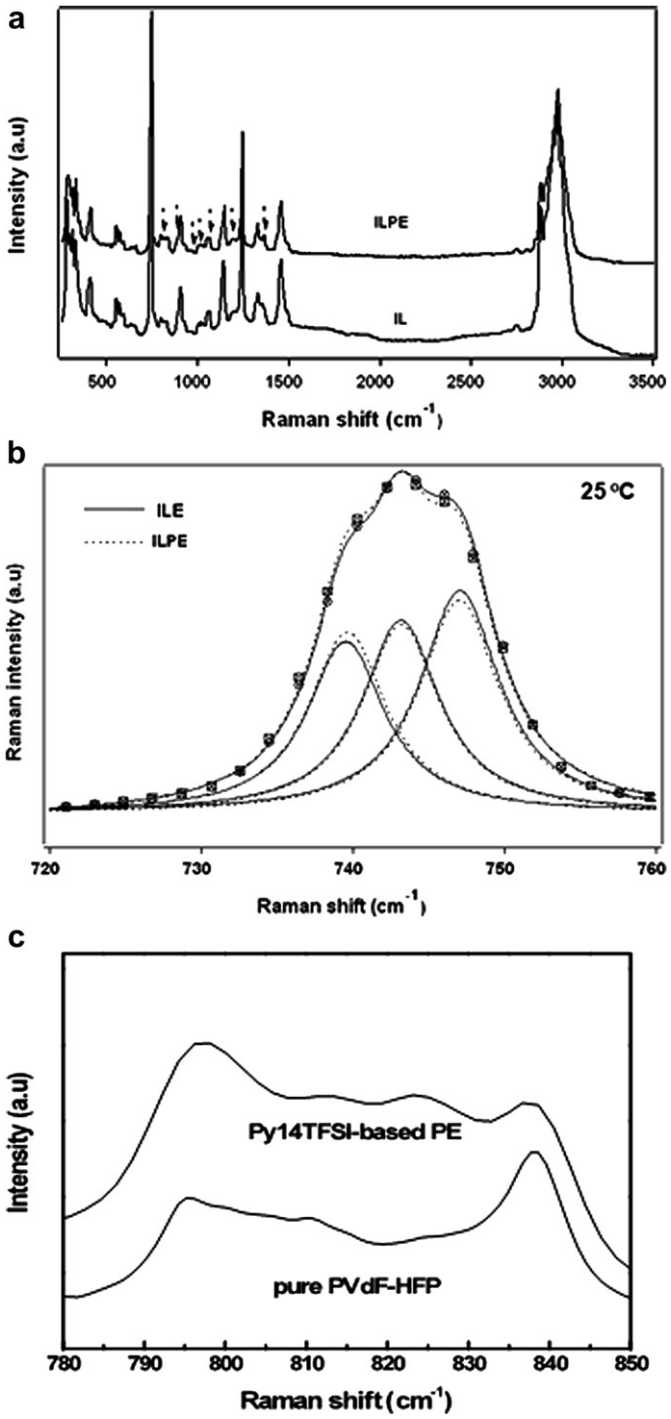


**Fig. 2.** (a) Room temperature Raman spectra of the $Py_{14}$TFSI ionic liquid electrolyte and the $Py_{14}$TFSI-based polymer electrolyte, (b) the symmetrical $CF_3$ bending mode for the two TFSI anion conformers (C1, C2) at ~739 $cm^{-1}$ and ~743 $cm^{-1}$, and TFSI coordination to Li ions at ~747 $cm^{-1}$ in the ILE and ILPE at 25 °C, (c) the combination mode of $CH_2$ rocking and $CF_2$ stretching in the PVdF-HFP membrane.

frequency range 720–760 $cm^{-1}$ at 25 °C. The solid and dotted component waves of the envelope correspond to band fits using Lorentzian profiles. This part of the Raman spectra is suitable to discuss the conformational isomerism of the $TFSI^-$ anion, since there is little overlap with Raman bands from $Py_{14}^+$ and this region is sensitive to both $Li^+$ coordinated TFSI and the conformational states of the $TFSI^-$ anion [30–32]. The contributions from the C1 (*cisoid*) and C2 (*transoid*) anion conformational states to the Raman

spectrum are observed at ~739 $cm^{-1}$ and ~743 $cm^{-1}$, respectively, and $Li^+$ coordinated TFSI give rise to the band at ~747 $cm^{-1}$. The $Li^+$ coordinated TFSI is unwanted, since it reduces the ionic conductivity of electrolytes and limits charge carrier mobility. With respect to the ILE spectrum, the C1 band of the ILPE is slightly more intense while the intensities for the C2 conformer are the same. From the intensities of the $Li^+$ coordinated TFSI, the concentration in the ILPE is slightly lower. However, the differences between the two electrolytes are small.

Raman spectra of the PVdF-HFP fibrous membranes are displayed in Fig. 2c. The band at ~795 $cm^{-1}$ is corresponding to the combination of $CH_2$ rocking ($\gamma$) and $CF_2$ stretching ($\nu$) in the $\alpha$ phase. The ~840 $cm^{-1}$ band is out of phase $\gamma CH_2$ and $\nu CF_2$ in the $\beta$ phase [33]. The ~795 $cm^{-1}$ band increases with soaking of the $Py_{14}$TFSI based ionic liquid electrolyte, which means that the $\beta$ phase is converted to $\alpha$ phase when the ILE is added. The decreased $\beta$ phase reduces the mechanical strength of PVdF-HFP, but also reduces the crystallinity and improves the conductivity.

The difference of ILE and ILPE on $Li^+$ ion mobility was observed by using solid state NMR. The $^7$Li NMR absorption spectra of ILE and ILPE are depicted in Fig. 3. A substantial decrease in the linewidth with ILPE is shown in Fig. 3, which indicates the increase in lithium mobility with the incorporation of PVdF-HHP membrane. $Li^+$ ion conduction could be confirmed by NMR study but the significant contribution of anion ($TFSI^-$) and $Py_{14}^+$ cation from ionic liquid to the total ionic conduction in the electrolyte is always possible.

Fig. 4 shows the DSC heating traces of ILE (a) and ILPE (b). On ILE, the exothermal peak around −30 °C and two endothermic peaks of −11.6 and 16.6 °C is indicating that the IL sample was not fully crystallized [34]. The ILPE exhibits two endothermic peaks at −80 °C and 0 °C, due to the glass transition and melting of the ILE, which were decreased in comparison with the ILE [21]. This observation confirms that the polymer matrix inhibits the phase transition of ILE. The crystallinity ($\chi_c$) of the PVdF-HFP membrane was calculated by normalizing the melting enthalpy ($\Delta H_m$) and by attributing a $\Delta H_{m.ref}$ according to the equation $\chi_c$ (%) = ($\Delta H_m$/$\Delta H_{m.ref}$) × 100. The electrospun PVdF-HFP membrane had a melting point at 159 °C with an estimated crystallinity of 74% based on a melting enthalpy of 104.7 J $g^{-1}$ ($\Delta H_{m.ref}$) for the fully crystalline polymer [7,35]. However, when electrospun membrane was soaked with the ionic liquid electrolyte, the melting temperature (94 °C) and degree of crystallinity (54%) were both decreased, which means that the amorphicity of the membrane increased.

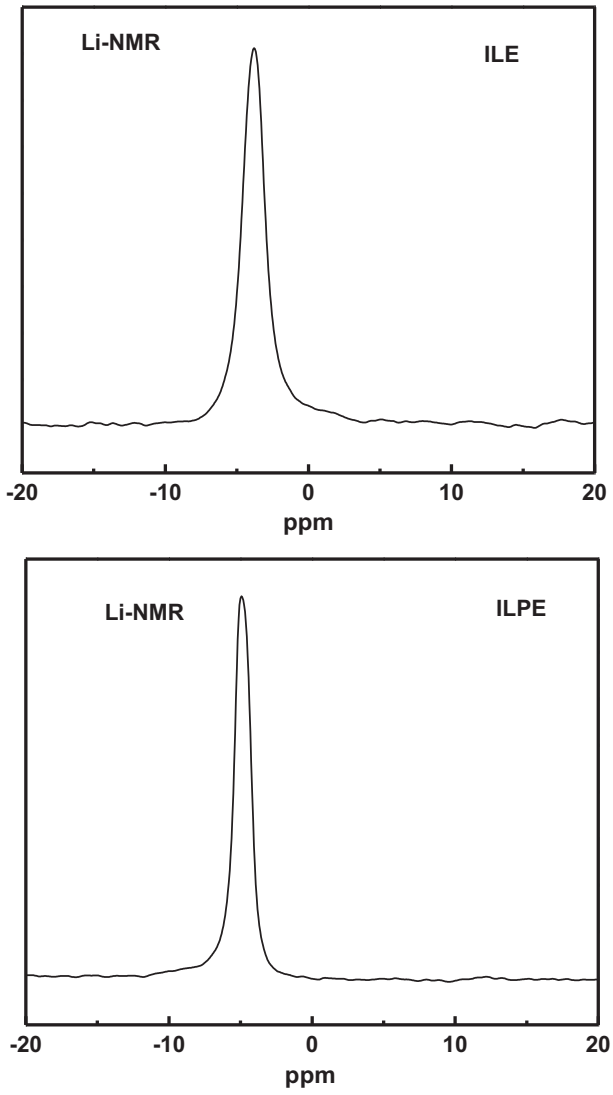


**Fig. 3.** $^7$Li NMR spectra for ILE and ILPE at room temperature.

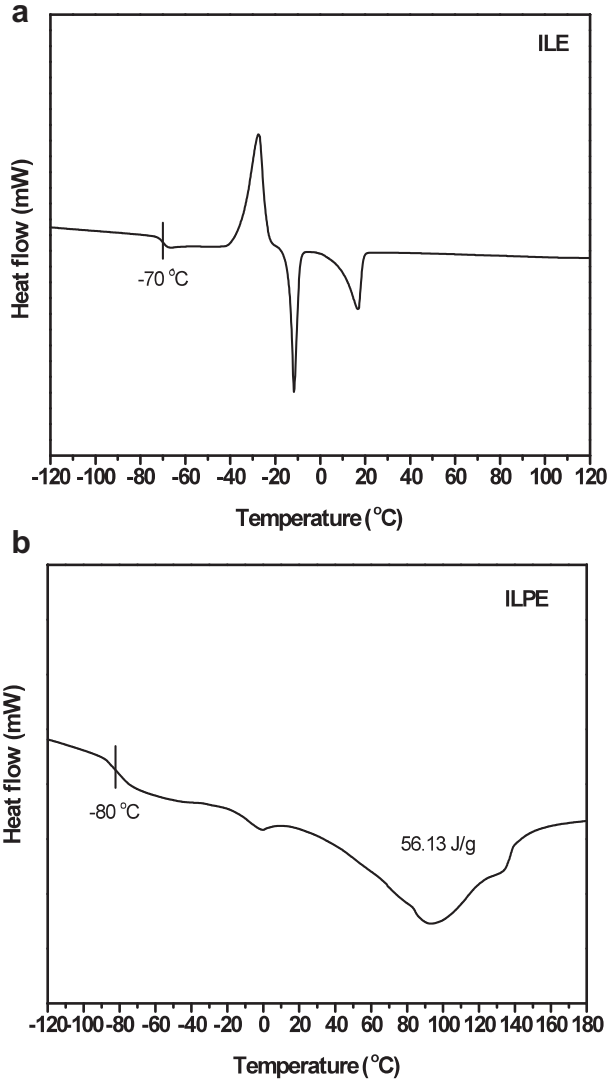


**Fig. 4.** DSC trace of $Py_{14}$TFSI-based ionic liquid electrolyte (ILE, a) and $Py_{14}$TFSI based polymer electrolyte (ILPE, b). Scan rate: 10 °C $min^{-1}$.

The lithium transport number of the ILE and ILPE were 0.05 and 0.04, respectively. Thus, we did not observe any significant improvement of the transference number in the ILPE. In contrast, there is a slight decrease of the transference number for the IL soaked polymer matrix. The lithium transference number is much lower than for commercial liquid electrolytes ($t_+ = \sim 0.3$ for 1 M LiTFSI in EC/DMC) due to strong interactions with the IL anions. Also, the low lithium transference number of ILEs was announced. Frömling et al. found $t_+ = 0.064$ for $(BMPTFSI)_{1-x}/(LiTFSI)_x$ at $x = 0.233$ [36], Saito et al. observed $t_+ = 0.027$ for BDMITFSI/LiTFSI at $x = 0.244$ [37] and Hayamizu et al. showed 0.045 in $EMIBF_4/LiBF_4$ [38].

The thermogravimetric analysis (TGA) results for ILPE in Fig. 5 indicate that the thermal degradation of ILPE occurs in two distinct stages. The results show an initial weight loss for ILPE below 100 °C, from which we conclude that the PVdF-HFP film is not completely free of moisture during TGA analysis. The first real weight loss and decomposition of the polymer complex occurs when the temperature gradually increases between 100 and 150 °C. The reason for this weight loss is scission of the main chains at weak head-to-head linkages [39]. The second decomposition takes place above 350 °C and is due to thermal degradation of both the ILE ( ~350 °C) and PVdF-HFP ( ~400 °C) units. The total weight loss for ILPE is 85%. The results suggest the ILPE to be thermally stable up to 350 °C in air atmosphere.

To ascertain the electrochemical stability of the ILPE, linear sweep voltammetry (LSV) measurements were made of laminated two electrode cells at room temperature. The ILPE result is presented in Fig. 6a. The working electrode potential of the cell was varied from 2.0 V to 8.0 V (versus Li) at a scan rate of 1 mV $s^{-1}$. No electrochemical reactions were found in the potential range 2.0–5.6 V. The onset of current flow at 5.6 V is associated with the decomposition of the ILPE. This result suggests that the ILPE is acceptable for high voltage cathode materials such as $LiCoO_2$, $LiCoPO_4$ and $LiMn_2O_4$ with in the absence of any catalytical effects. Moreover, the oxidation stability of ILPE is higher than ILE in around 0.5 V as a result of the block effect of polymer matrix.

Cyclic voltammograms (CV) of the Li/ILPE/Li cell are presented in Fig. 6b. The redox peaks in the initial cycle correspond to anodic oxidation at +0.16 V and a cathodic reduction at −0.16 V vs. $Li^+/Li$. No shifts of the anodic and cathodic voltages were observed during cycling. The quantity of charge transferred decreased in the second cycle, but the cell showed nearly overlapping CV curves after the first two cycles, indicating highly reversible redox processes with high columbic efficiency.

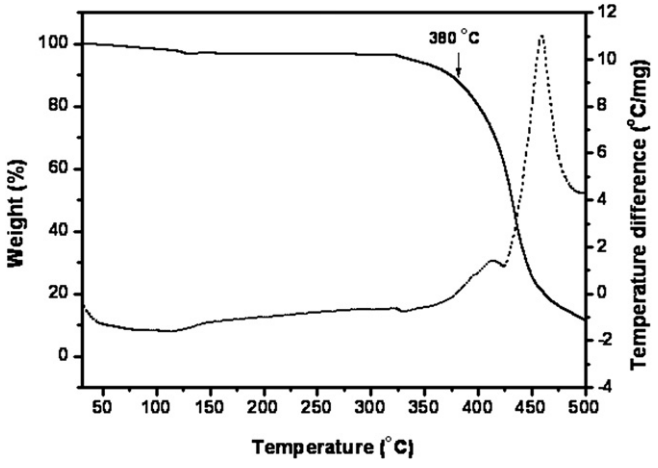


**Fig. 5.** TGA trace of the $Py_{14}TFSI$-based polymer electrolyte (ILPE) in air atmosphere. Scan rate: 10 °C $min^{-1}$.

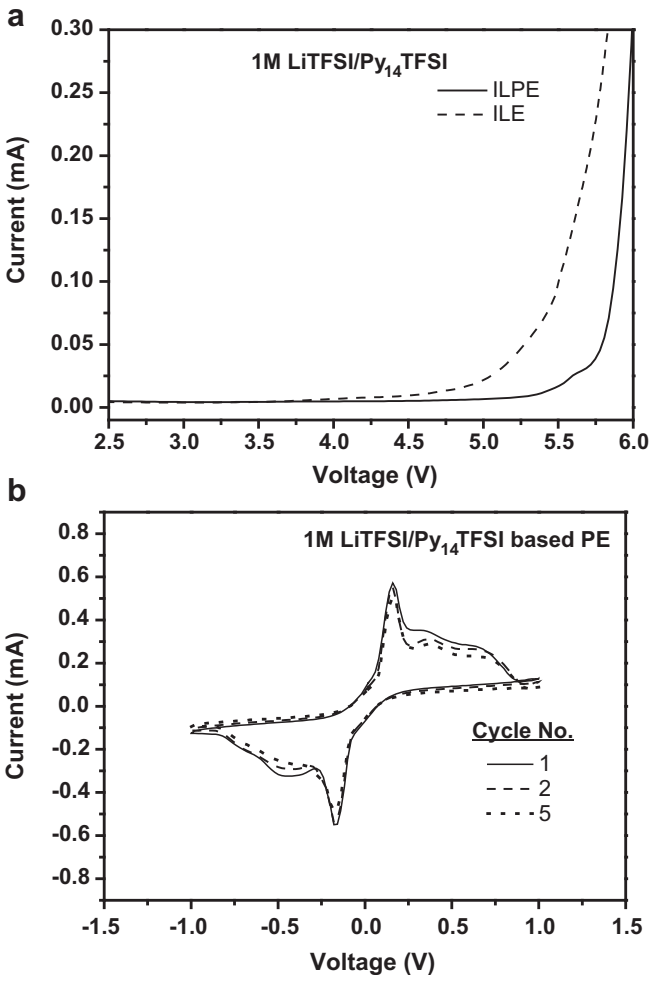


**Fig. 6.** (a) Linear sweep voltammetry (LSV) plots of an SS/Li cell with the $Py_{14}TFSI$-based polymer electrolyte (ILPE), (b) cyclic voltammetry (CV) curves of the 1st, 2nd and 5th cycles of the $Py_{14}TFSI$ based polymer electrolyte (ILPE) in a Li half cell at 25 °C. Scan rate: 1 mV $s^{-1}$.

The galvanostatic charge–discharge curves of the $LiFePO_4$/ILPE/Li cell, cycled five times between 2.5 and 4.0 are shown in Fig. 7a. The $LiFePO_4$ cell demonstrated a single charge–discharge plateau at 3.47 and 3.39 V versus $Li/Li^+$, which reflects the low cell resistance that remains stable during cycling. During the first charging process at 0.1 C-rate the voltage increased sharply to 3.47 V from the open circuit voltage (OCV = 3.4 V). A flat long plateau followed, gradually increasing to the cut-off voltage and a capacity of 142 mA h $g^{-1}$. The discharge curve shows one plateau region for the ILPE cell, which means that there are no impurities effecting the electrochemical reactions. The irreversible capacity loss between the first charge and discharge reaction was less than 3 mA h $g^{-1}$ giving almost 99% columbic efficiency for $LiFePO_4$. However, a large voltage separation ($\Delta V$) and low discharge capacity (115 mA h $g^{-1}$) was observed at 1 C-rate, because of the high viscosity [40,41].

The cycling performance of the Li/ILPE/$LiFePO_4$ cell at room temperature under 0.1 and 1 C-rates is presented in Fig. 7b. The cell shows stable cycling performance at 0.1 C over the 55 cycles made in this work. One can see that, except for the initial three cycles, the cell cycled with an initial capacity of 143 mA h $g^{-1}$ and retained excellent capacity retention of 92% at room temperature. The discharge capacity fade for the Li/ILPE/$LiFePO_4$ cell calculated on basis of the initial and 55th cycle capacities is ~0.16% per cycle at 0.1 C. Although the capacity fade is increased at 1 C-rate, the

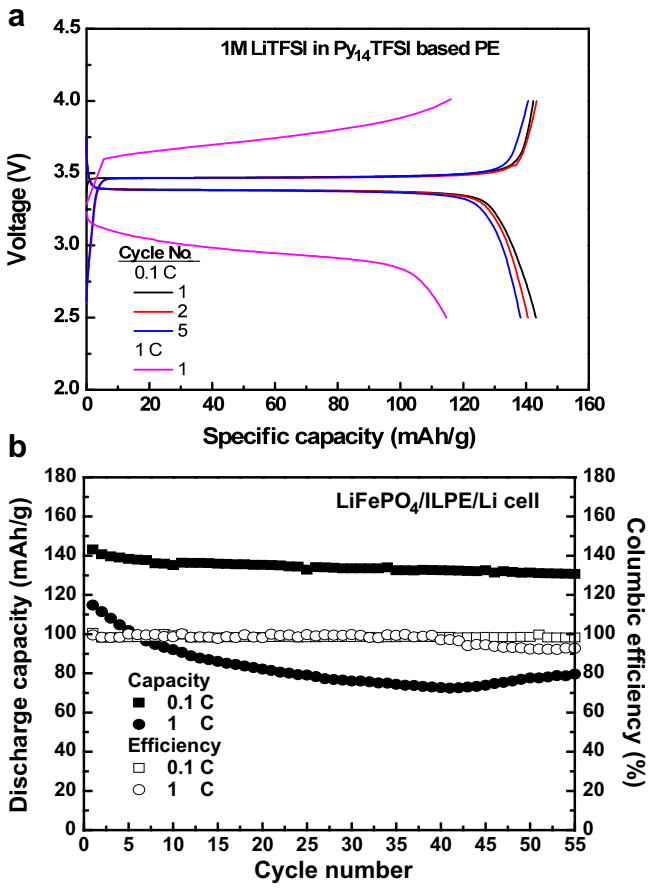


**Fig. 7.** First, second, and fifth cycle charge–discharge capacities (a) and cycle performance (b) of a Li/$LiFePO_4$ cell with the $Py_{14}$TFSI-based polymer electrolyte (ILPE) (25 °C, 0.1 and 1 C-rate, 2.5–4.0 V).

capacity retention is still above 69% after 55 cycles. The good cycle ability of ILPE is because it might be hypothesized diffusion of the ILE mixture from ILPE to the composite cathode to form a stable ternary blend with the PVdF binder in electrode. The Li/ILPE/$LiFePO_4$ cell also exhibit a good columbic efficiency at both current density but the columbic efficiency is decreased at high current density after 40-cycle due to the dendrite formation on lithium anode. The good cycling performance of the cell is promising and reflects a combination of thermal and electrochemical stability of the ionic liquid electrolyte and excellent conduction properties.

## 4. Conclusions

In this work an electrolyte combining the ionic liquid $Py_{14}$TFSI with an electrospun PVdF-HFP polymer host shows excellent physical and electrochemical properties, such as: weak $Li^+$ coordination to TFSI, low crystallinity, high ionic conductivity, high thermal and electrochemical stability, and good compatibility with a $LiFePO_4$ electrode. Also, a $LiFePO_4$/Li cell with this electrolyte exhibits good cycling performance. Therefore, this ionic liquid-based polymer electrolyte is found to be suitable for application in high safety lithium batteries.

## Acknowledgements

The present work was supported by STINT and KRF in a joint Korea–Sweden program, FORMAS and the Chalmers Area of Advance – Energy.

## References

[1] J.M. Tarascon, M. Armand, Nature 414 (2001) 359.
[2] D.E. Fenton, J.M. Parker, P.V. Wright, Polymer 14 (1973) 589.
[3] M. Armand, Solid State Ionics 9/10 (1983) 745.
[4] J.M. Tarascon, A.S. Gozdz, C. Schmutz, F. Chmutz, F. Shokoohi, P.C. Warren, Solid State Ionics 86–88 (1996) 49.
[5] M. Walkowiak, A. Zalewska, T. Jesionowski, M. Pokora, J. Power Sources 173 (2007) 721.
[6] X. Li, G. Cheruvally, J.-K. Kim, J.-W. Choi, J.-H. Ahn, K.-W. Kim, H.-J. Ahn, J. Power Sources 167 (2007) 491.
[7] S.-W. Choi, S.-W. Jo, W.-S. Lee, Y.-R. Kim, Adv. Mater. 15 (2003) 2027.
[8] J.-K. Kim, G. Cheruvally, X. Li, J.-H. Ahn, K.-W. Kim, H.-J. Ahn, J. Power Sources 178 (2008) 815.
[9] P. Wasserscheid, W. Keim, Angew. Chem. Int. 39 (2000) 3772.
[10] M. Armand, F. Endres, D.R. MacFarlane, H. Ohno, B. Scrosati, Nat. Mater. 8 (2009) 621.
[11] D.R. MacFarlane, J. Sun, J. Golding, P. Meakin, M. Forsyth, Electrochim. Acta 45 (2000) 1271.
[12] J.-H. Shin, W.A. Henderson, G.B. Appetecchi, F. Alessandrini, S. Passerini, Electrochim. Acta 50 (2005) 3859.
[13] S. Randström, G.B. Appetecchi, C. Lagergren, A. Moreno, S. Passerini, Electrochim. Acta 53 (2007) 1837.
[14] A. Lewandowski, A. Swiderska-Mocek, J. Power Sources 194 (2009) 601.
[15] J.-K. Kim, G. Cheruvally, J.-W. Choi, J.-U. Kim, J.-H. Ahn, G.-B. Cho, K.-W. Kim, H.-J. Ahn, J. Power Sources 166 (2007) 211.
[16] B. Scrosati, J. Garche, J. Power Sources 195 (2010) 2419.
[17] C. Sirisopanaporn, A. Fernicola, B. Scrosati, J. Power Sources 186 (2009) 490.
[18] A. Fernicola, F.C. Weise, S.G. Greenbaum, J. Kagimoto, B. Scrosati, A. Soleto, J. Electrochem. Soc. 156 (2009) A514.
[19] E. Abitelli, S. Ferrari, E. Quartarone, P. Mustarelli, A. Magistris, M. Fagnoni, A. Albini, C. Gerbaldi, Electrochim. Acta 55 (2010) 5478.
[20] G.-T. Kim, G.B. Appetecchi, M. Carewaka, M. Joost, A. Balducci, M. Winter, S. Passerini, J. Power Sources 195 (2010) 6130.
[21] G.B. Appetecchi, G.-T. Kim, M. Montanino, M. Carewska, R. Marcilla, D. Mecerreyes, I.D. Meatza, J. Power Sources 195 (2010) 3668.
[22] J.-K. Kim, J.-W. Choi, G. Cheruvally, J.-U. Kim, J.-H. Ahn, G.-B. Cho, K.-W. Kim, H.-J. Ahn, Mater. Lett. 61 (2007) 3822.
[23] P. Bruce, C. Vincent, J. Electroanal. Chem. 225 (1987) 1.
[24] G.Z. Żukowska, M. Marcinek, S. Drzewiecki, J. Kryczka, J. Syzdek, A. Adamczyk-Woźniak, W. Wieczorek, A. Sporzyński, J. Power Sources 195 (2010) 7506.
[25] P.G. Bruce, J. Evans, C.A. Vincent, Solid State Ionics 28 (1988) 918.
[26] Y. Aihara, G.B. Appetecchi, B. Scrosati, J. Electrochem. Soc. 149 (2002) A849.
[27] J.-H. Shin, P. Basak, J.B. Kerr, E.J. Cairns, Electrochim. Acta 54 (2008) 410.
[28] B. Rupp, M. Schmuck, A. Balducci, M. Winter, W. Kern, Eur. Polym. J. 44 (2008) 2986.
[29] V. Aravindan, P. Vickraman, K. Krishnaraj, Polym. Int. 57 (2008) 932.
[30] S. Duluard, J. Grondin, J.-L. Bruneel, I. Pianet, A. Grélard, G. Campet, M.-H. Delville, J.-C. Lassègues, J. Raman Spectrosc. 39 (2008) 627.
[31] I. Rey, P. Johansson, J. Lindgren, J.-C. Lassègues, J. Grondin, L. Servant, J. Phys. Chem. A 102 (1998) 3249.
[32] J.-K. Kim, A. Matic, J.-H. Ahn, P. Jacobsson, J. Power Sources 195 (2010) 7639.
[33] A. Martinelli, M.A. Navarra, A. Matic, S. Panero, P. Jacobsson, L. Börjesson, B. Scrosati, Electrochim. Acta 50 (2005) 3992.
[34] W.A. Henderson, S. Passerini, Chem. Mater. 16 (2004) 2881.
[35] P. Raghavan, J.-W. Choi, J.-H. Ahn, G. Cheruvally, G.S. Chauhan, H.-J. Ahn, C. Nah, J. Power Sources 184 (2008) 437.
[36] T. Frömling, M. Kunze, M. Schönhooff, J. Sundermeyer, B. Roling, J. Phys. Chem. B 112 (2008) 12985.
[37] Y. Saito, T. Umecky, J. Niwa, T. Sakai, S. Maeda, J. Phys. Chem. B 111 (2007) 11794.
[38] K. Hayamizu, Y. Aihara, H. Nakagawa, T. Nukuda, S.W. Price, J. Phys. Chem. B 108 (2004) 19527.
[39] N. Katsikis, F. Zahradnik, A. Helmschrott, H. Miinstedt, A. Vital, Polym. Degrad. Stab. 92 (2007) 1966.
[40] H.F. Xiang, B. Yin, H. Wang, H.W. Lin, X.W. Ge, S. Xie, C.H. Chen, Electrochim. Acta 55 (2010) 5204.
[41] Z.P. Rosol, N.J. German, S.M. Gross, Green Chem. 11 (2009) 1453.